

Optical variability of unidentified Active Galactic Nuclei with blazar characteristics in the *Fermi*-2LAC catalogue

L. Klindt*†

Department of Physics, University of the Free State, Bloemfontein, 9301, South Africa

E-mail: lizelkeklindt@gmail.com

B. van Soelen

Department of Physics, University of the Free State, Bloemfontein, South Africa

E-mail: vansoelenb@ufs.ac.za

P.J. Meintjes

Department of Physics, University of the Free State, Bloemfontein, South Africa

E-mail: meintpj@gmail.com

A. de Witt

Hartebeesthoek Radio Astronomy Observatory, Hartebeesthoek, South Africa

E-mail: alet@hartrao.ac.za

BL Lacartae objects (BL Lacs) and flat spectrum radio quasars (FSRQs) exhibit variability in the continuum flux at multiple wavelengths on timescales of hours to days. We report on optical photometric observations of 8 unidentified Active Galactic Nuclei (AGN) from the second *Fermi*-LAT catalogue of AGN, that shows potential blazar characteristics. We mainly focus our attention on the intra-day variability (IDV) with timescales of a few minutes to within a day and the short term variability (STV) on timescales of a few days to months. Variability on these timescales are known to be the result of the shock zones within the jet, hot spots and/or instabilities in the accretion disk. Preliminary differential photometric results, for the 8 target sources, obtained with the SAAO 1.9-m Sutherland High-Speed Optical Camera (SHOC) during December 2014 and May 2015, are discussed. Currently, optical long term monitoring of the entire target sample using the Watcher Robotic Telescope is undertaken to determine magnitudes in the *RVi* filters, as well as radio observations with the the HartRAO 26-m radio telescope to construct light curves in order to study the variability.

3rd Annual Conference on High Energy Astrophysics in Southern Africa -HEASA2015,

18-20 June 2015

University of Johannesburg, Auckland Park, South Africa

*Speaker.

†This paper uses observations made at the South African Astronomical Observatory (SAAO).

1. Introduction

The Large Area Telescope (LAT) onboard the *Fermi* Gamma-ray Space Telescope spacecraft has been operational since August 2008. The LAT covers 20% of the sky at any instant and has an energy range of 20 MeV to 300 GeV [1]. The *Fermi*-LAT 2-year Source catalogue (2LAC) consists of a clean sample¹ of 866 gamma-ray sources located at high galactic, of which approximately 157 of these sources were classified as AGN of unknown type (AGU) with no determined redshifts [2]. We have identified a subset of these AGUs with blazar characteristics (see section 2) for further multi-wavelength analysis that included optical spectroscopic and photometric observations with the Southern African Large Telescope (SALT) and the SAAO 1.9-m telescope, as well as single-dish radio observations with the HartRAO 26-m telescope. Here we report on the optical photometric results obtained for 8 unclassified *Fermi*-2LAC targets in our sample.

Blazars are active galaxies with a supermassive black hole (SMBH) at the centre surrounded by an accretion disc that accumulates material from the host elliptical galaxy. These highly energetic sources are believed to be driven by the SMBH from which a relativistic jet, directed close to our line of sight, originates and expands to kiloparsec scales. Blazars are classified into BL Lactertae (BL Lac) and Flat-spectrum Radio Quasars (FSRQs), and are characterised by rapid variability at multi-wavelength, high polarization from radio to optical wavelengths and Doppler-boosted multi-wavelength emission originating from the jet, making these sources spectacular astronomical laboratories to study particle acceleration and a variety of multi-wavelength radiation mechanisms.

The Spectral Energy Distributions (SEDs) of blazars are well known for their "double-humped" shape with a low-energy component extending from radio to UV/X-rays, and a high-energy component that extends from X-rays to GeV/TeV gamma-rays. Synchrotron emission from relativistic electrons gives rise to the low-energy component, whereas the processes involved at high energies are still under debate, and both leptonic and hadronic processes are considered (see e.g. [3]). The leptonic model supports External Compton (EC) scattering of photons from the accretion disc, dust torus or Broad Line region, or Synchrotron Self Compton (SSC) scattering of photons produced by the synchrotron emission in the jet. The hadronic model alternatively states that the emission of the high energy component is produced by the decay of π^0 mesons to photons, pair cascades or synchrotron and Compton emission from secondary charged pions [4, 5, 6, 7].

BL Lac objects and FSRQs exhibit continuum flux variability at multiple wavelengths on timescales of hours to years. Based on the timescales three variability classes arises, namely intra-day (IDV), short-term (STV) and long-term (LTV) variability. In these proceedings we focus on the IDV with timescales of a few minutes to within a day, and STV which vary on timescales from days to months [8]. The sources of the intrinsic short-term variability are the shocks within the jet, hot spots and instabilities in the accretion disk, while the binary black hole model accounts for the long-term periodic variability [9]. The Shock-in-Jet Model states that flux variability is caused either by the interaction of the shock with irregularities as it propagates down the jet [10], or by the variability in the direction of the relativistic shocks to the line of sight [11]. Models based on

¹Some of the AGN are affected by analysis issues (flagged), while other sources are associated with multiple AGN (26 sources for example have two possible associations). Therefore, a clean sample is constructed comprising of sources which have a firm analytical measurement.

disturbances in the accretion disk explain IDV of blazars in a low-state when the contribution of the jet is weak, which allows one to study the accretion disk [12].

2. Sample selection

We have originally selected 19 AGUs in the *Fermi*-2LAC catalogue based on criteria previously employed by [15] in their search for blazar candidates amongst sources listed in the third EGRET source catalogue. We have only selected high galactic sources ($|b| > 10^\circ$) which are observable from southern latitudes ($-90^\circ \leq \delta \leq +35^\circ$) and fall within the magnitude limit of $V_{mag} \leq 21$ (fainter targets are excluded from the sample due to observational limitations). The selected targets exhibit gamma-ray photon indices in the range of $1.2 < \Gamma < 3$ (see e.g. Figure 12 in [2]) and are bright enough in the radio regime to be observable with the HartRAO 26-m telescope ($S_{4.85 \text{ GHz}} \geq 100 \text{ mJy}$). We also considered the *Fermi*-LAT variability index to determine the probability for a source to be variable, though this was not used as a strict selection criterion. Sources with a variability index greater than 41.6 have a 99% chance to be variable over the two year observation period [2, 15, 16]. All the targets with the exception of 2FGL J2040.2-7109 lacked redshift measurements (z). For a full discussion of the selection criteria and the original target list see [17].

From the original target list we have focused on undertaking multi-wavelength follow-up observations of 10 blazar-like targets with the specific aim of determining the unknown properties of these sources and classify them accordingly to their multi-wavelength behaviour (see [18] for the original target list). These selected sources are all still identified as AGU in the recently released 3FGL catalogue [19].

3. Observations and data reductions

The optical photometric observations and data analysis undertaken with the SAAO 1.9-m telescope are summarized below.

3.1 Optical photometric observations

We have utilised the Sutherland High-Speed Optical Camera (SHOC) mounted on the SAAO 1.9-m telescope to obtain differential photometry of the 8 targets listed in Table 1. Our observations were carried out in the clear passband during August and December 2014, and May 2015, with the exception of two targets for which we also have obtained B and V passband data during May 2015. We used the clear filter for this program to determine whether IDV and STV variability are indeed present in the target, with the exception of 2FGL J1218.8-4827 and 2FGL J1955.0-5639 for which we have also obtained V and B filter data. Each target was observed on timescales of 1–3 hours per night depending on its visibility, over a period of 3 to 6 nights, with exposure times ranging from 10 sec to 4 min. We took care to select a field of view with at least two comparison stars available for corrections.

<i>Fermi</i> -2LAC Name	<i>V</i> mag	RA _{J2000}	Dec _{J2000}	Γ	<i>S</i> _{4.85}	Passband
2FGL J0044.7-3702	19.60	00:45:12	-37:05:49	2.57	330	C
2FGL J0201.5-6626	20.56	02:01:08	-66:38:13	2.25	168	C
2FGL J0644.2-6713	20.69	06:44:28	-67:12:57	2.16	218	C
2FGL J0730.6-6607*	15.13	07:30:50	-66:02:19	1.34	82	C
2FGL J0855.1-0712	19.78	08:55:09	-07:15:03	2.62	1157	C
2FGL J1218.8-4827*	17.53	12:19:02	-48:26:28	2.40	65	C, B, V
2FGL J1955.0-5639*	17.25	19:55:03	-56:40:29	1.88	9	C, B, V
2FGL J2040.2-7109	17.47	20:40:08	-71:14:52	2.03	481	C

Table 1: Candidate AGUs in the *Fermi*-2LAC catalogue with blazar characteristics which have been observed with SHOC. The radio counterparts within the 95% error circle are listed with their corresponding *V*-magnitude position, gamma-ray photon index (Γ) and radio flux density at 4.85 GHz (*S*_{4.85}). The passband of the photometric observations undertaken with SHOC is also indicated. The three targets indicated with an asterisk did not meet the radio flux density criteria, but are still included in the sample since these targets satisfy the rest of the selection criteria.

3.2 Data reductions and differential photometry

The SHOC pipeline, based on python and IRAF packages, was used to reduce the raw photometric data.² The pipeline splits each data cube into separate frames, applies bias and flat field corrections, and runs standard aperture photometry performed with optimum apertures. The instrumental magnitudes of the target and comparisons were corrected by considering weighted differential photometry where the weighted average instrumental magnitude $\langle m_j \rangle$ of the comparison stars is computed for each frame by (see e.g. [21, 22])

$$\langle m_j \rangle = \frac{\sum_{k=1}^K m_{kj} \omega_k}{\sum_{k=1}^K \omega_k}, \quad (3.1)$$

with,

$$\omega_k = \frac{1}{\langle m_{err,k}^2 \rangle}, \quad (3.2)$$

where k is the running number of the comparison star, K the number of comparison stars, j the frame number, m_{kj} the magnitude of the k -th comparison star in the j -th frame, and m_{err} the mean theoretical error of the measured magnitude m_k given by IRAF. The mean magnitude M of all comparison stars averaged over all frames is given by

$$M = \frac{\sum_{j=1}^N \langle m_j \rangle}{N}, \quad (3.3)$$

where N is the number of frames. The difference between the weighted average magnitude $\langle m_j \rangle$ of the comparison stars and the mean magnitude M of all comparison stars averaged over all frames are then subtracted from the observed magnitude of the target

$$m_{cor,ij} = m_{ij} - (\langle m_j \rangle - M), \quad (3.4)$$

where $m_{cor,ij}$ and m_{ij} are respectively the corrected and initial magnitudes of star i in frame j .

²see <http://shoc.saao.ac.za/Documents/ShocnHelpful.pdf> for manual and <http://www.saao.ac.za/~marissa/SHOCpipeline/> for pipeline instructions.

4. Variability statistical analysis

Previous searches for IDV have relied on statistical tests such as the C-test, F-test and power-enhanced F-test (see e.g. [23, 24, 25, 26]). However, several problems with these tests have been pointed out in studies done by e.g. [27, 28, 29]. We therefore considered different approaches done by different groups. Here we have used the F-test and the power-enhanced F-test, performed at the $\alpha = 0.01$ (2.6σ) and $\alpha = 0.001$ (3σ) significance levels, to search for IDV and STV. Further investigations are currently conducted to sufficiently detect the presence of variability in blazar-like sources by considering the errors within the data sample as done by e.g. [30].

4.1 F-test

We have employed the F-statistics given by [23] as shown below:

$$F_1 = \frac{\text{Var}(B - s_1)}{\text{Var}(s_1 - s_2)}, \quad F_2 = \frac{\text{Var}(B - s_2)}{\text{Var}(s_1 - s_2)}, \quad (4.1)$$

where $\text{Var}(B - s_1)$, $\text{Var}(B - s_2)$ and $\text{Var}(s_1 - s_2)$ are the variances in the magnitude of the blazar-star₁, blazar-star₂ and star₁-star₂ differential lightcurves (DLCs), respectively. F_1 , F_2 and the average F-value, F_{avg} , were then compared separately with the critical F-value, $F_{\nu_B \nu_{ss}}^{(\alpha)}$, where ν_B and ν_{ss} are the degrees of freedom of the blazar-star and the star-star DLCs, respectively. The degrees of freedom are the same for the blazar-star and star-star DLCs for the F-test, and can be obtained with $n = N - 1$, where N is the number of frames. Targets where F_1 , F_2 and F_{avg} have a confidence larger than 0.99 were regarded as variable (V); targets where only two of the three F-values have a confidence larger than 0.99 were regarded as possible variable (PV); and targets where the confidence is less than 0.99 for all three F-values, were regarded as non-variable (N).

4.2 Power-enhanced F-test

The limitations to claim variability detection in blazars with the F-test are discussed by [28]. One needs to consider statistics with an increased number of degrees of freedom in the denominator of the F-distribution to increase the power of the test. This can be accomplished by stacking all the light curves of the comparison stars and transforming the comparison star DLCs to match the mean magnitude of the target. Here we entailed the method utilized by [28, 29]. The degrees of freedom of the target and the comparison stars were determined with $n = N - 1$ and $m = k(N - 1)$, respectively, where N is the number of frames and k is the number of comparison stars. The critical F-value was then obtained from F-distribution tables for confidence levels of $\alpha = 0.01$ and $\alpha = 0.001$. We compared the F_{enh} value with the critical F-statistics, and we claimed variability if the F_{enh} value was greater than the critical value for both $\alpha = 0.01$ and $\alpha = 0.001$. For a F_{enh} value greater than the critical value for both significance levels $\alpha = 0.01$ and less than the critical value for $\alpha = 0.001$, we considered the target to be possibly variable. And if the F_{enh} value is less for both confidence levels the target was regarded as non-variable (N).

5. Results

We report here specifically on the STV and IDV of 8 unclassified *Fermi*-2LAC AGN sources with SHOC, as discussed below.

Target name	F ₁	F ₂	F _{avg}	F _{crit,α=0.01}	F _{crit,α=0.001}	Status	F _{enh}	F _{crit,α=0.01}	F _{crit,α=0.001}	Status
J0044.7-3702	0.50	0.67	0.59	2.26	2.98	N, N, N	1.35	1.95	2.42	N
J0201.5-6626	2.87	1.56	2.21	1.37	1.53	V, V, V	5.93	1.31	1.43	V
J0644.2-6713	1.86	2.39	2.13	1.33	1.46	V, V, V	4.91	1.28	1.38	V
J0730.6-6607	9.02	9.25	9.13	1.68	2.00	V, V, V	23.59	1.68	2.00	V
J0855.1-0712	0.24	1.12	0.68	1.32	1.45	N, N, N	0.64	1.27	1.37	N
J1218.8-4827	5.29	4.56	4.92	1.68	1.98	V, V, V	17.93	1.68	1.98	V
J1955.0-5639	0.98	0.14	0.56	2.46	3.36	N, N, N	0.28	2.08	2.64	N

Table 2: Short term variability of 7 unclassified *Fermi*-2LAC AGN sources. The F-test values and power-enhanced F-test values determined for each target are displayed with the indication whether the test states variability or not. V=variable, i.e., confidence > 0.997; PV=probable variable, i.e., 0.99 – 0.997 confidence; N =non-variable, i.e., confidence < 0.99.

5.1 Short term variability

The DLCs for our target sample are shown in Figures 1 to 7, with the exception of 2FGL J2040.2-7109 that was only observed for one night. The DLCs are obtained in clear filter except for 2FGL J1218.8-4827 and 2FGL J1955.0-5639 for which we obtained *B* filter observations on short term timescales. We executed the different variability tests and the results are summarized in Table 2. For 3 targets, namely 2FGL J0044.7-3702, 2FGL J0855.1-0712 and 2FGL J1955.0-5639, STV is rejected by all the statistical tests, whereas for the rest of our sample we have detected variability.

5.2 Intra-day variability

We observed each target over a series of nights for 1-3 hours per night (depending on the target’s track length) in order to detect IDV in the clear filter, with the exception of 2FGL J1218.8-4827 and 2FGL J1955.0-5639 which we also observed in the *B* and *V* filters. In Figures 8 to 15 we present DLCs on IDV timescales for each target. The different variability statistics were also employed for the IDV and the results are listed in Table 3. All three test results correlate well with each other.

6. Multi-wavelength campaign

Multi-wavelength observations are fundamental to investigate blazars in all their complexity. In addition to the optical photometric observations discussed above, we have also obtained spectra for 7 targets with the SAAO 1.9-m telescope and the SALT. Long term optical monitoring is also on-going with the Watcher Robotic telescope at Boyden in *VRi* filters [31].

Archival searches within the Catalina Real Time Survey (CRTS)³ have been obtained in order to determine potential correlations between the CRTS and *Fermi*-LAT light curves. One of our sources, 2FGL J0644.2-6713, shows potential long term correlation (observations from 2006 to 2012) between the optical and the gamma-ray regimes as shown in Figure 16.

Radio observations at 5 and 8.4 GHz are currently being undertaken with the HartRAO 26-m telescope to determine the detectability and the flux densities of the sources. Within the *Fermi*

³<http://nesssi.cacr.caltech.edu/DataRelease/>

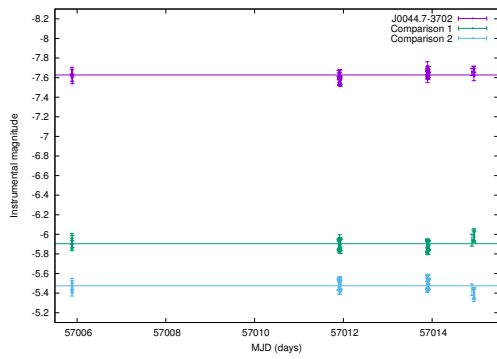


Figure 1: DLC of 2FGL J0044.7-3702 taken over the nights of 14, 20, 22 and 23 December 2014 in clear filter.

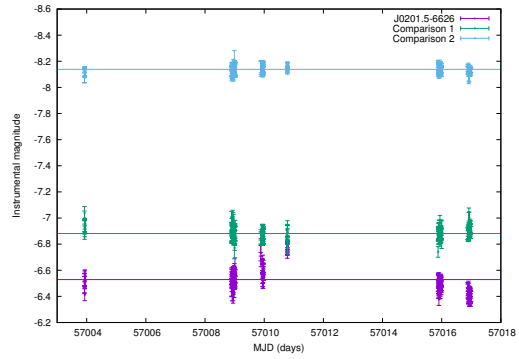


Figure 2: DLC of 2FGL J0201.5-6626 taken over the nights of 12, 17, 18, 19, 24 and 25 December 2014 in clear filter.

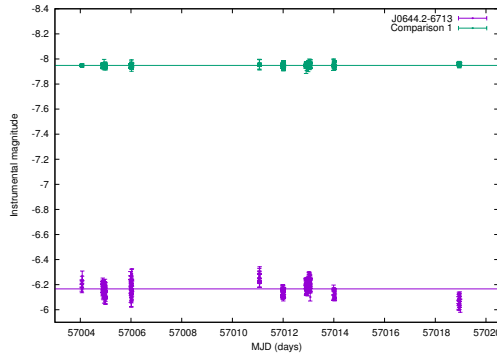


Figure 3: DLC of 2FGL J0644.2-6713 taken over the nights of 12, 13, 14, 19, 20, 21, 22 and 27 December 2014 in clear filter.

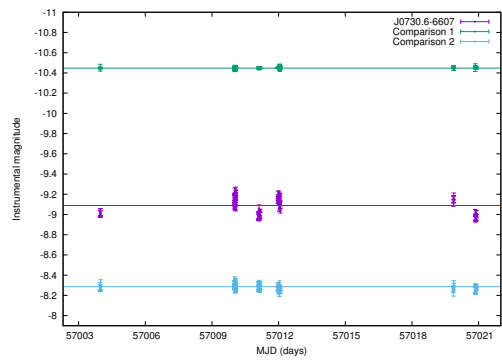


Figure 4: DLC of 2FGL J0730.6-6607 taken over the nights of 12, 18, 19, 20, 28 and 29 December 2014 in clear filter.

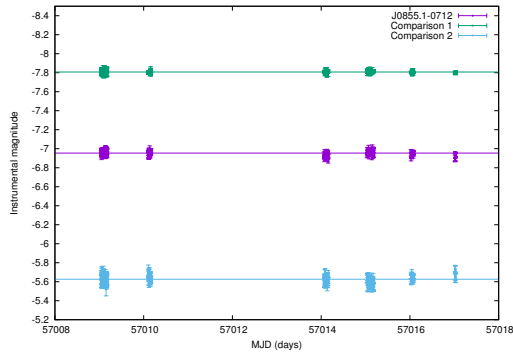


Figure 5: DLC of 2FGL J0855.1-0712 taken over the nights of 17, 18, 22, 23, 24 and 25 December 2014 in clear filter.

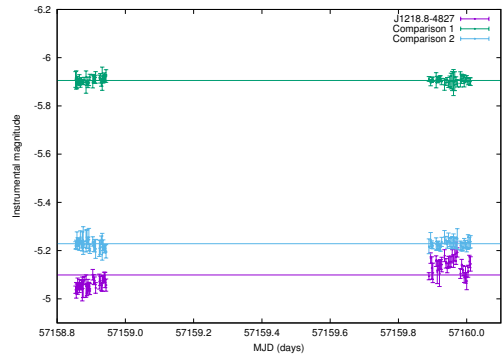


Figure 6: DLC of 2FGL J1218.8-4827 taken over the nights of 16 and 17 May 2015 in *B* filter.

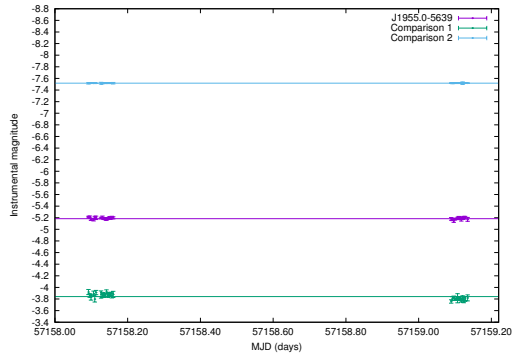


Figure 7: DLC of 2FGL J1955.0-5639 taken over the nights of 15 and 16 May 2015 in *B* filter.

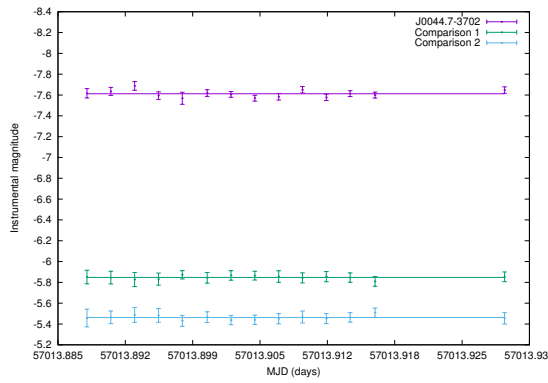


Figure 8: IDV lightcurve of 2FGL J0044.7-3702 taken 22 December 2014 in clear filter.

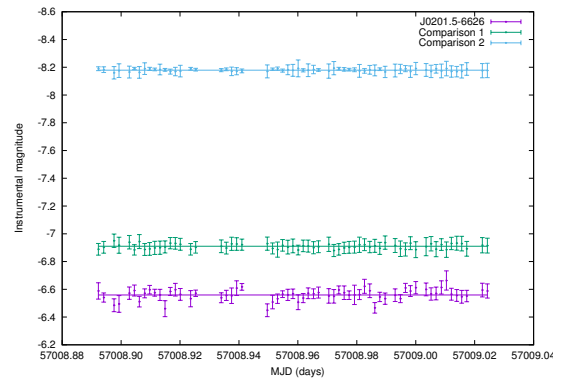


Figure 9: IDV lightcurve of 2FGL J0201.5-6626 taken 17 December 2014 in clear filter.

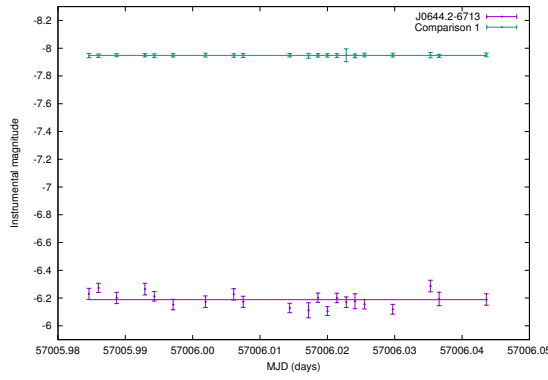


Figure 10: IDV lightcurve of 2FGL J0644.2-6713 taken 14 December 2014 in clear filter.

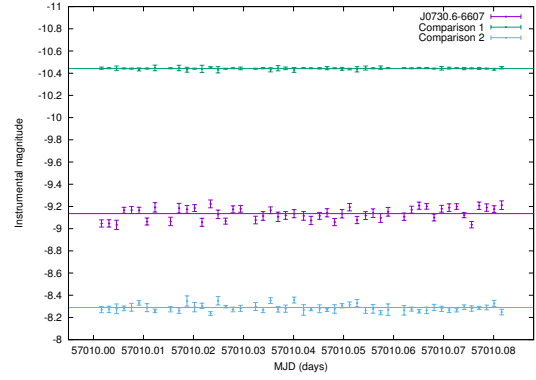


Figure 11: IDV lightcurve of 2FGL J0730.6-6602 taken 18 December 2014 in clear filter.

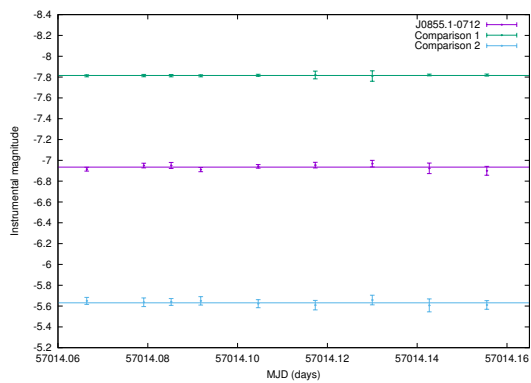


Figure 12: IDV lightcurve of 2FGL J0855.1-0712 taken 22 December 2014 in clear filter.

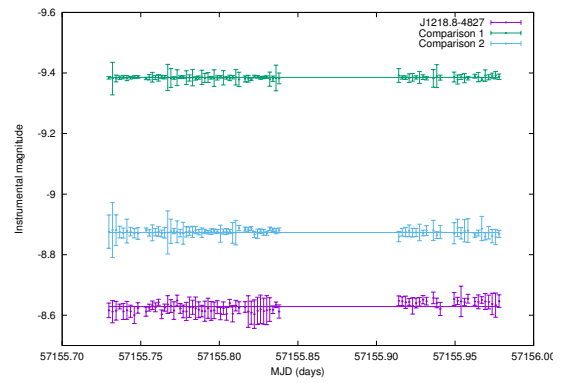


Figure 13: IDV lightcurve of 2FGL J1218.8-4827 taken 16 May 2015 in clear filter.

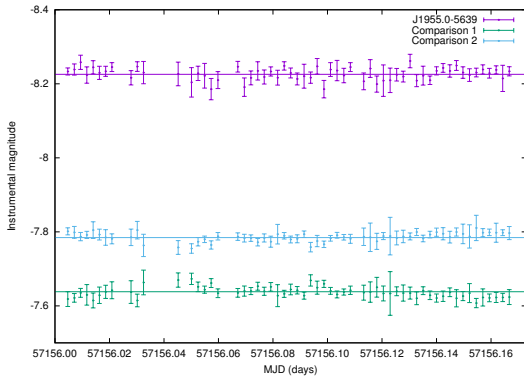


Figure 14: IDV lightcurve of 2FGL J1955.0-5639 taken 13 May 2015 in clear filter.

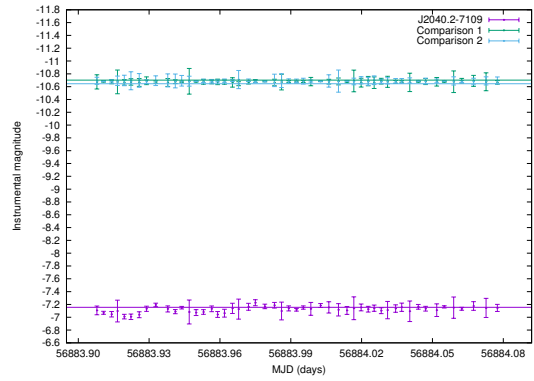


Figure 15: IDV lightcurve of 2FGL J2040.2-7109 taken 14 August 2014 in clear filter.

2LAC potential radio counterparts are given for the AGU targets and flux measurements in the radio band have been obtained from surveys such as the Green Bank 6-cm (GB6), Parkes-MIT-NRAO (PMN) Survey, etc. We only include sources which are potentially observable with the HartRAO 26-m telescope, and our first trial run was to determine whether the sources included are radio “bright” enough to be detected with the HartRAO single dish. These observations will form the basis of a proposed long term monitoring campaign to establish the radio variability and flux densities of the candidate sources. This will provide additional constraints for the SEDs to model and classify the sources. Similar work to undertake single-dish radio observations with the HartRAO 26-m telescope was also employed by [15] in a previous study of unidentified EGRET sources. In their study they reported on flux density measurements of PKS J0820-5705 and PMN J0710-3850 at 18 cm, 13 cm, 6 cm, 5 cm, 4.5 cm, 3.5 cm and 2.5 cm, which contributed to their multi-wavelength campaign to classify these EGRET sources of unknown type as a FSRQ and a LINER, respectively.

7. Discussion and Conclusion

The optical photometric results obtained with SHOC mounted on the SAAO 1.9-m telescope show promising results with STV detected over a timescale of a week for 4 targets in our *Fermi*-2LAC AGU sample. The statistical tests rejected STV for 2FGL J0044.7-3702, 2FGL J0855.1-0712 and 2FGL J1955.0-5639. We found that for most nights the targets listed in our sample do not exhibit IDV with exception of 2FGL J0201.5-6626, 2FGL J0644.2-6713, 2FGL J0730.6-6607 and 2FGL J1218.8-4827, which show possible variability and/or variability in the clear filter over a series of nights. We are investigating the efficiency of variability detection with the modified F-test and power-enhanced F-test, and it is important to note that these two tests correlate well with each other. However, further analysis regarding different statistical tests is ongoing.

Optical long term monitoring with the Watcher Robotic Telescope is also currently being undertaken. We intend to search for correlations between these data and other wavelength regimes, as well as study color-correlations within the optical band itself and investigate a variety of unknown properties such as estimating an upper mass limit on the SMBH.

Target name	Obs date	Filter	F-test status	Power-enhanced F-test status
J0044.7-3702	14/12/2014	C	N, N, N	N
J0044.7-3702	20/12/2014	C	N, N, N	PV
J0044.7-3702	22/12/2014	C	N, N, N	N
J0044.7-3702	23/12/2014	C	N, N, N	PV
J0201.5-6626	12/12/2014	C	N, N, N	N
J0201.5-6626	17/12/2014	C	V, V, V	V
J0201.5-6626	18/12/2014	C	V, V, V	V
J0201.5-6626	19/12/2014	C	N, N, N	N
J0201.5-6626	24/12/2014	C	V, V, V	V
J0201.5-6626	25/12/2014	C	N, N, N	V
J0644.2-6713	12/12/2014	C	N, N, N	N
J0644.2-6713	13/12/2014	C	PV, N, N	V
J0644.2-6713	14/12/2014	C	V, V, V	V
J0644.2-6713	19/12/2014	C	PV, N, PV	PV
J0644.2-6713	20/12/2014	C	N, N, N	V
J0644.2-6713	21/12/2014	C	N, N, N	V
J0644.2-6713	22/12/2014	C	N, N, N	N
J0644.2-6713	27/12/2014	C	N, N, N	N
J0730.6-6607	12/12/2014	C	V, PV, PV	V
J0730.6-6607	18/12/2014	C	V, V, V	V
J0730.6-6607	19/12/2014	C	N, N, N	PV
J0730.6-6607	20/12/2014	C	N, N, N	N
J0730.6-6607	28/12/2014	C	V, V, V	V
J0730.6-6607	29/12/2014	C	N, N, N	PV
J0855.1-0712	17/12/2014	C	N, N, N	N
J0855.1-0712	18/12/2014	C	N, N, N	N
J0855.1-0712	22/12/2014	C	N, N, N	N
J0855.1-0712	23/12/2014	C	N, N, N	N
J0855.1-0712	24/12/2014	C	N, N, N	N
J0855.1-0712	25/12/2014	C	N, N, N	N
J1218.8-4827	13/05/2015	C	V, V, V	V
J1218.8-4827	16/05/2015	V	N, N, N	V
J1218.8-4827	16/05/2015	B	N, N, N	N
J1218.8-4827	17/05/2015	B	V, N, PV	V
J1955.0-5639	15/09/2014	C	N, PV, N	N
J1955.0-5639	13/05/2015	C	N, N, N	V
J1955.0-5639	15/05/2015	B	N, N, N	N
J1955.0-5639	16/05/2015	B	N, N, N	N
J2040.2-7109	14/09/2014	C	V, V, V	V

Table 3: IDV of 8 unclassified *Fermi*-2LAC AGN sources. The results of the F-test and power-enhanced F-test determined for each target are displayed with the indication whether the test states variability or not. V = variable, i.e., confidence >0.997; PV = probable variable, i.e., 0.99 – 0.997 confidence; N = non-variable, i.e., confidence <0.99.

We have detected potential correlation between the CRTS *V*-magnitude LC and *Fermi*-LAT LC over a long term timescale for 2FGL J0644.2-6713. Simultaneous, multi-wavelength, long-term monitoring campaigns are therefore needed to directly compare the behavior of the target at different frequencies. We are also undertaking single-dish radio test observations with the HartRAO 26-m telescope to establish source detectability at 5 and 8.4 GHz with the HartRAO 26-m telescope, for potential long-term monitoring of the targets at multiple radio frequencies.

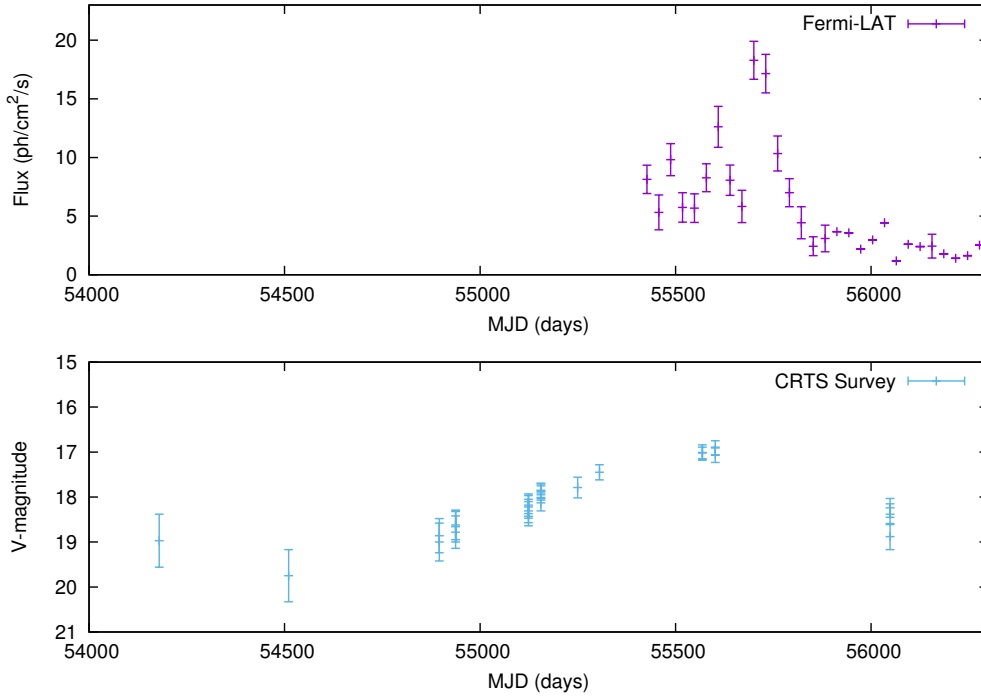


Figure 16: Potential long term correlation between the optical V-magnitude (CRTS data) and gamma-ray flux (*Fermi*-LAT data) of 2FGL J0644.2-6713.

8. Acknowledgements

The financial assistance of the National Research Foundation (NRF) towards this research is hereby acknowledged. This work is based on the research supported in part by the National Research Foundation of South Africa for the grant 87919. Any opinion, finding and conclusion or recommendation expressed in this material is that of the authors and the NRF does not accept any liability in this regard. This paper uses observations made at the South African Astronomical Observatory (SAAO).

References

- [1] A.B. Atwood et al., *Fermi/Large Area Telescope Bright Gamma-ray Source List*, *ApJ* **697** (2009) 071
- [2] M. Ackermann et al, *The second catalog of Active Galactic Nuclei detected by the Fermi Large Area Telescope*, *ApJ* **171** (2011) 37
- [3] M. Böttcher, A. Reimer, K. Sweeney and A. Prakash, *Leptonic and Hadronic Modeling of Fermi-detected blazars*, *ApJ* **768** (2013) 54
- [4] K. Mannheim and P.L. Biermann, *Gamma-ray flaring of 3C 279: a proton initiated cascade in the jet?*, *A&A* **253** (1992) L21
- [5] F.A. Aharonian, *TeV Gamma Rays from BL Lac Objects due to Synchrotron Radiation of Extremely High Energy Photons*, *NewA*, **5** (2000) 377

- [6] A. Mücke and R.J. Protheroe, *A proton synchrotron blazar model for flaring in Markarian 501*, *Aph* **15** (2001) 121
- [7] A. Mücke, R.J. Protheroe, R. Engel, J.P. Rachen and T. Stanev, *BL Lac objects in the synchrotron proton blazar model*, *Aph* **18** (2003) 593
- [8] S.J. Wagner and A. Witzel, *Intraday Variability In Quasars and BL Lac Objects*, *ARA&A* **33** (1995) 163
- [9] A.C. Gupta et al., *Periodic Oscillations in the Intra-Day Optical Light Curves of the Blazar S5 0716+714*, *ApJ* **690** (2009) 216
- [10] A.P. Marscher et al., *Multi-frequency VLA, VLBI and Single-dish Observations of the Quasar 4C 39.25*, *ApJ* **371** (1991) 491
- [11] Gopal-Krishna and P.J. Wiita, *Gaseous halos of elliptical galaxies, the cosmic evolution of their radio sizes, and the phenomenon of compact steep-spectrum sources*, *ApJ* **373** (1991) 325
- [12] A.V. Mangalam and P.J. Wiita, *Accretion disk models for optical and ultraviolet microvariability in active galactic nuclei*, *ApJ* **406** (1993) 420
- [13] J.L. Richards et al., *Precise γ -ray Timing and Radio Observations of 17 Fermi γ -ray Pulsars*, *ApJ* **194** (2011) 29
- [14] J.L. Richards et al., *Probing interstellar extinction near the 30 Doradus nebula with red giant stars*, *MNRAS* **438** (2014) 30
- [15] P. Nkundabakura and P.J. Meintjes, *Unveiling the nature of two unidentified EGRET blazar candidates through spectroscopic observations*, *MNRAS* **427** (2012) 859
- [16] P.L. Nolan et al., *Fermi Large Area Telescope Second Source Catalog*, *ApJ* **199** (2011) 31
- [17] L. Klindt, P.J. Meintjes and B. van Soelen, *Multi-wavelength classification of unidentified AGN in the Fermi-2LAC catalogue*, *Proceedings of SAIP* (2014) 341
- [18] L. Klindt, B. van Soelen, P.J. Meintjes and P. Väisänen, *Optical spectroscopic observations of unclassified Active Galactic Nuclei in the Fermi-2LAC catalogue*, *Proceedings of SAIP 2015*, submitted
- [19] F. Acero et al., *Fermi Large Area Telescope Third Source Catalog*, *ApJ*, arXiv:1501.02003 (2015)
- [20] M. Ackermann et al., *The Third Catalog of Active Galactic Nuclei Detected by the Fermi Large Area Telescope*, *ApJ* arXiv:1501.06054 (2015)
- [21] A.Y. Burdanov, V.V. Krushinsky and A.A. Popov, *Astrokit - an efficient program for high-precision differential CCD photometry and search for variable stars*, *AstBu* **69** (2014) 368
- [22] M. Everett and S.B. Howell, *A Technique for Ultrahigh-Precision CCD Photometry*, *PASP* **113** (2001) 1428
- [23] R. Joshi et al., *Optical microvariability properties of BALQSOs*, *MNRAS* **412** (2011) 2717
- [24] H. Gaur et al., *Optical Flux and Spectral Variability of Blazars*, *MNRAS* **425** (2012) 3002
- [25] A. Goyal, *Intra-night optical variability of core dominated radio quasars: the role of optical polarization*, *A&A*, arXiv: 1205.2324 (2012)
- [26] A. Agarwal and A.C. Gupta, *Multiband optical variability studies of BL Lacartae*, *MNRAS* **450** (2015) 541

- [27] J.A. de Diego, *Testing Tests on Active Galactic Nuclei Microvariability*, *ApJ* **139** (2010) 1269
- [28] J.A. de Diego, *On the reliability of microvariability tests in quasars*, *astro-Ph*, arXiv:1409.0468 (2014)
- [29] H. Gaur et al., *Nature of Intra-night Optical variability of BL Lacartae*, *MNRAS* **452** (2015) 4263
- [30] A. Goyal et al., *Improved characterization of intra-night optical variability of prominent AGN classes*, *MNRAS* **435** (2013) 1300
- [31] M. Topinka et al., *Status update of the Watcher Robotic Telescope*, *EAS Publication Series* **61** (2013) 487